

# Theoretical Notes

Note 196

SLL-74-0218

Unlimited Distribution

Printed April 1974

QUICKE2: A One-Dimensional Code for  
Calculating Bulk and Vacuum Emitted  
Photo-Compton Currents

Theodore A. Dellin  
Analytical Division 8341  
Sandia Laboratories, Livermore

Crawford J. MacCallum  
Theoretical Division 5223  
Sandia Laboratories, Albuquerque

## ABSTRACT

The theory and operational features of the one-dimensional code QUICKE2 are described. The code calculates the bulk and vacuum-emitted photo-Compton current of electrons generated in a material exposed to photons with energies from 1 keV to 10 MeV and arbitrary angle of incidence. The rapid and easy-to-use calculational technique is based on analytical solutions to the transport equation modeling electron multiple scattering and slowing down.



## Contents

	<u>Page</u>
I. Introduction	I-1
A. Future Developments	I-2
II. Problem Geometry	II-1
A. Bulk Currents	II-1
B. Emission Currents	II-3/4
III. Theory	III-1
A. Bulk	III-1
B. Vacuum Emission	III-4
B.1. Quantum Efficiency	III-9
B.2. Angular Distribution	III-11
B.3. Energy Distribution	III-12
B.4. Surface Energy Deposition and Low Energy Secondary Electrons	III-13/14
IV. Computational Details	IV-1
Appendix I - Material Data	AI-1
Appendix II - Input Cards	AII-1
Appendix III - Output Information	AIII-1
Appendix IV - Sample Problem	AIV-1

References



## I. Introduction

QUICKE2 is a FORTRAN code for computing the photo-Compton current (PCC) of electrons generated in a one-dimensional material irradiated with a plane wave of photons. The electron flux is driven along with the photon flux, continually generated by Compton and photoelectric processes and continually brought to rest by the stopping power of the medium. QUICKE2 considers two problems using different calculational techniques. The first problem is the prediction of the PCC in the bulk of a material (more than one electron range from any interface). These bulk PCC are given by exact solutions of the transport equation modeling primary electrons.<sup>1</sup> The second problem is the prediction of the number, energy and angular distribution of electrons photo-emitted into vacuum as well as the energy deposition at the material/vacuum interface. Vacuum PCC are expressed in terms of the exact bulk calculations by an approximate solution to the transport equation.<sup>2,3</sup> The code is rapid and easy to use. Predictions based on the results of the code agree with the available experimental data as well as the more detailed Monte Carlo codes, except in extreme cases. A compilation of the bulk PCC predictions has already been published.<sup>4</sup> The purpose of making the code available is to allow the user to predict vacuum emission, PCC for additional materials, and PCC produced by photon spectra.

The material considered is a homogeneous mixture composed of any subset of a group of 25 of the more commonly occurring elements whose photon and electron cross sections are stored on a data tape. The bulk current predictions are valid more than one electron range from any interface, independent of the shape of the material. The vacuum PCC refer to emission from the front or back surface of a one-dimensional slab whose thickness is greater than the range of the most energetic electrons created by the photon flux of interest.

The elementary photon source considered is a monoenergetic plane wave. The code calculates responses to photon spectra by superposition. The photon energy range is from 1 keV to 10 MeV. Bulk PCC can be calculated at an arbitrary angle with respect to the photon direction. The magnitude, energy distribution integrated over angle, and surface energy deposition of vacuum PCC can be evaluated for photons incident at an arbitrary angle with respect to the surface normal. The complete emission angular distribution can be calculated for normally incident photons. The angular distribution can also be calculated for non-normal incidence provided the photon source or electron detector has azimuthal symmetry. Secondary photons (Compton scattered, fluorescence and bremsstrahlung) are not considered.

The sources of electrons are Compton, photoelectric and Auger processes. Pair production has charge/anticharge symmetry and is not considered. Secondary knock-on electrons are also not included in the calculation. A semi-empirical value for the magnitude of vacuum-emitted low-energy (<50 eV) electrons is given for certain metals. The electron elastic scattering cross sections and stopping powers are taken from the SANDYL code.<sup>5</sup>

In Section II, the problem geometry is defined. The bulk and vacuum interface methods are discussed in Section III. Section IV describes the computational organization of QUICKE2. Appendix I considers the material data used. Appendix II describes the input cards while Appendix III describes the output. A sample problem is provided in Appendix IV.

#### A. Future Developments

Extensions of the capabilities of the QUICKE2 code are in progress. A data tape containing all 100 elements with improved low-energy electron-nuclear scattering cross sections will be made available. A version of the code that more accurately predicts back emission from low atomic number materials is being developed. Analytical formulae for the PCC at the interfaces between different materials will be incorporated into future versions allowing the calculation of the non-local energy and charge depositions at interfaces. We also plan to publish additional handbooks describing vacuum and interface PCC.

## II. Problem Geometry

The geometry considered in the calculations is shown in Figure 1. A one-dimensional homogeneous material is exposed in vacuum to a monoenergetic photon flux. The surface nearer the photon source is called the back surface and the surface farther from the photon source is called the fore surface. The outward surface normal of the fore surface is taken as the reference direction. The photon direction is defined by the angle of incidence,  $\theta_0$ , with respect to this reference direction. For the monoenergetic photon flux the range of the most energetic electron ( $\leq$  photon energy) can be determined. The bulk of the material is defined as the locus of all points whose distance from any surface is greater than this maximum electron range. For a fixed geometry the size of the bulk will depend on the photon energy. QUICKE2 does not calculate photon attenuation. It is assumed that the user knows the photon flux at the bulk or surface point of interest.

### A. Bulk Currents

Several components of the bulk PCC are calculated in QUICKE2. The basic quantity is the net current along the reference direction, Figure 1(a). This net current may be resolved into a fore current of electrons traveling in the positive direction, Figure 1(b), and a back current of electrons traveling in the negative direction, Figure 1(c). Finally, the "fore"="back" current of electrons crossing a plane whose normal is perpendicular to the reference direction is also calculated, Figure 1(d). (If  $\theta_0 \neq 0$ , an azimuthal average is understood.) The bulk PCC are expressed as ratios of the electron/photon fluxes. The units are electrons/photon which is equivalent to  $[\text{electrons}/(\text{cm}^2\text{sec})]/[\text{photon}/(\text{cm}^2\text{sec})]$ . The user is reminded that as the photon beam traverses the bulk of the material, the photon flux is attenuated. The absolute magnitude of the bulk PCC is proportionally decreased and this divergence of the electron flux leads to the generation of a bulk charge density. Furthermore, if a photon spectrum is considered the relative spectrum will change with position because generally the lower energy photons

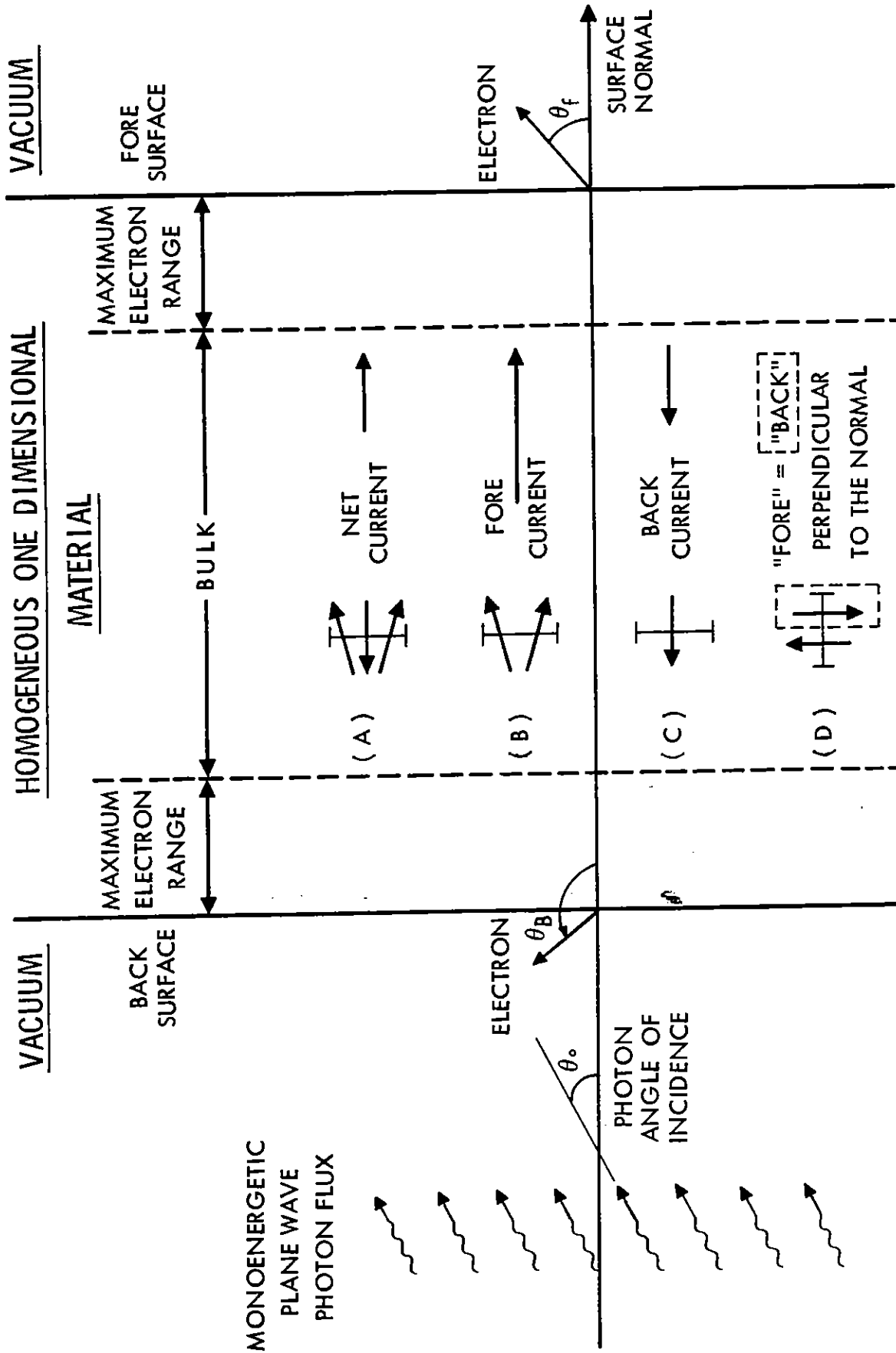


Figure 1 - Problem Geometry



are attenuated more. Photon attenuation is negligible over distances of the order of an electron range, but for greater thickness the effects of photon attenuation may be important.

### B. Emission Currents

For the vacuum photoemission calculations the material need only be one electron range thick. Again the results are expressed as ratios of electron/ photon fluxes with the photon flux at either surface assumed know. The magnitude of the electron flux emitted from the surface is measured in units of (electrons/photon) which is equivalent to units of (electrons  $\text{cm}^{-2} \text{sec}^{-1}$ )/ (photon  $\text{cm}^{-2} \text{sec}^{-1}$ ). The angular distribution integrated over all energies is given in units of (electrons/photon/degree) or (electrons/photon/steradian) the two being related by

$$\frac{dN}{d\theta} = \frac{\pi^2}{90} \left| \sin\theta \right| \frac{dN}{d\Omega}$$

where  $\theta$  is the angle of the emitted electron with respect to the outward surface normal of the fore surface.  $\theta$  varies from 0 to 90° at the fore surface and from 90° to 180° at the back surface. The energy distribution integrated over all angles is given in units of (electrons/photon/MeV).

In some applications the source is a narrow-beam, rather than a plane wave of photons. In these cases, the total number of vacuum photoemitted electrons is required rather than the surface density of emitted electrons. For normal incidence, the ratio of electrons/photons is the same for a plane wave or a thin beam. However, for non-normal incidence, there is a difference because as the sample is tilted the areal density of photons striking the material for a plane wave source decrease proportional to  $\cos\theta_0$  while in the narrow-beam case the total number of photons intercepting the material is constant. Therefore, to predict total photoemission results for a narrow-beam geometry, the surface density results generated by QUICKE2 should be multiplied by  $\sec \theta_0$ .



### III. THEORY

#### A. Bulk

The calculations of the bulk PCC are based upon an analytic solution to the transport equation describing electron transport in a medium.<sup>1</sup> Whereas the solution to these equations for the general case requires Monte Carlo solution procedures, analytic solutions are possible if the simplifications listed in Table I are introduced. With the exception of Item A in Table I, these simplifications apply for the majority of practical problems. The method provides an exact solution for the transport equation modeling primary electrons in the bulk of a material.

The theory of PCC calculations is treated in detail in Reference 1. The following outline, however, gives the basic elements of the calculations.

A beam of electrons injected into an unbounded medium with residual range  $s_0$  and direction cosine  $\mu_0$  with respect to the z-axis will have, after slowing down to a residual range  $s \leq s_0$ , a distribution of direction cosines  $\mu$  given by

$$G(s_0, \mu_0; s, \mu) = \sum_{n=0}^{\infty} (n+\frac{1}{2}) P_n(\mu_0) P_n(\mu) e^{-\int_s^{s_0} \kappa_n(s') ds'} \quad (1)$$

This is the well-known Goudsmit-Saunderson distribution in which the  $P_n$  are Legendre polynomials and  $\kappa_n$  is the nth scattering transport cross section:

$$\kappa_n(s) \equiv \int_{-1}^1 \sigma(\mu, s) [1 - P_n(\mu)] du \quad (2)$$

In this relation,  $\sigma(\mu, s)$  is the single scattering electron cross section.

TABLE I  
SIMPLIFICATIONS TO TRANSPORT IN THE BULK

Simplification	Comment
A. The point of observation is in a homogeneous medium and is more than an electron range from any boundary.	This simplification is addressed in the next section.
B. The photon flux is spatially uniform over an electron range.	The photon mean free path generally exceeds the range of electrons it generates by at least an order of magnitude.
C. The "continuous-slowing-down-approximation" is an adequate model of energy loss.	This approximation is widely used in electron transport calculations and its validity is generally supported by Monte Carlo experience.
D. The medium is field-free.	This approximation is valid in most solids because (1) the stopping power of the medium dominates any electric field effects at fields less than $10^5$ V/cm and (2) the cyclotron radius of an electron in a magnetic field is usually large compared to the electron's range.
E. Secondary electrons and photons do not contribute significantly to the PCC.	Monte Carlo calculations indicate that secondary- and higher-order electrons and photons contribute less than 10% to PCC over the ranges of Z and $h\nu$ considered here.

Given a spatially uniform and time-independent source of electrons distributed in residual range and direction cosine according to some function  $S(s_0, \mu_0)$ , during time  $\delta t$  the number of electrons crossing area  $\delta A$  normal to the z-axis in the forward direction must be

$$J_F \delta A \delta t = \int_0^\infty ds_0 \int_{-1}^1 d\mu_0 S(s_0, \mu_0) \int_0^{s_0} n(s_0, s) ds \int_0^1 d\mu \mu v(s) \delta t \delta A G(s_0, \mu_0; s, \mu) \quad (3)$$

in which  $v(s)$  is the velocity corresponding to residual range  $s$  and  $n(s_0, s)$  is the steady-state distribution of residual ranges produced by a constant unit source with initial value  $s_0$ . By conservation arguments, this distribution must be just  $v^{-1}(s)$  for  $s \leq s_0$ . Using Equation (1) and Equation (3), the forward current is then

$$J_F = \int_0^\infty ds_0 \int_{-1}^1 d\mu_0 S(s_0, \mu_0) \sum_{n=0}^\infty R_n(s_0) P_n(\mu_0) \alpha_n \quad (4)$$

in which

$$\alpha_n \equiv (n + \frac{1}{2}) \int_0^1 \mu P_n(\mu) d\mu \quad (5)$$

and

$$R_n(s_0) \equiv \int_0^{s_0} ds e^{-\int_s^{s_0} \kappa_n(s') ds'} \quad (6)$$

The expression for the backward current,  $J_B$ , is the same except that the limits on the integral defining  $\alpha_n$  are 0 and -1. For the net current,  $J_N$ , the limits are -1 and 1, so that only  $\alpha_1 = 1$  is not zero.

The  $R_n(s_0)$  are a set of generalized projected ranges of which  $R_0 = s_0$  is the full residual range and  $R_1$  is the mean vector range projected along the initial electron direction. The ratio  $R_1/R_0$ , which might be called the "fractional forward-directed range," varies smoothly with energy and  $Z$  and is a convenient measure of multiple scattering effects.

These equations and cross sections describe completely the electron currents produced by an arbitrary source  $S$ . It remains only to relate the source term  $S$  to the photon fluence.

Energetic electrons are produced by three principal photon interaction processes: Compton scattering, photoelectric absorption, and Auger emission from an excited atom. Pair production has almost symmetric particle/anti-particle transport and therefore contributes very little to the bulk currents. It does contribute to energy deposition and to surface emission experiments which distinguish positrons from electrons. For photon energies exceeding  $30 Z^{-1/2}$  MeV, pair production exceeds 1/3 of the total interaction cross section and these QUICKE2 results should be used with care. Compton interactions are described by the Klein-Nishina cross section for the interaction of photons and free electrons.<sup>6</sup> Auger emission from K- and L-shells is modeled using decay probabilities from the review paper by Bambynek, et al.<sup>7</sup> and the photoelectric cross-section compilations of Biggs.<sup>8</sup> Since Auger emission is isotropic, these electrons contribute equally to the forward and backward currents but do not contribute to the net current.

Total photoelectric cross sections are taken from the analytical formulae of Biggs. The net current is calculated using the accurate initial photoelectric electron angular distributions from the PELEC Code of Brysk and Zerby.<sup>9</sup> The forward and back bulk PCC are calculated with the simpler angular distributions of Fischer and Sauter as discussed in Reference 1.

#### B. Vacuum Emission

The vacuum emission calculations are based on a generalization of a calculational procedure due to Weymouth<sup>10</sup> to obtain analytical solutions for the PCC in the vicinity of a one-dimensional vacuum interface. The analytical solutions are possible if the simplifications in Table II are introduced. The simplifications for the emission calculations are more extensive than for the bulk calculations. Indeed, it would seem that some of the simplifications are quite severe. We find, however, that the method can be made to yield results of surprising generality, simplicity and accuracy.

The mathematical details of the method are given in Reference 3. The following outline briefly describes the theory as originally formulated by Weymouth and then describes our improvements.

TABLE II  
SIMPLIFICATIONS TO TRANSPORT AT A VACUUM INTERFACE

Simplification	Comment
A. Simplifications B-E from Table I.	See Table I.
B. Vacuum emission is calculated at the front or back surface of a one-dimensional homogeneous material whose thickness is greater than or equal to the maximum electron range generated.	The range of electrons generated by 1 keV - 10 MeV photons in solids are usually small compared to practical dimensions. Furthermore, these one-dimensional results can be used to generate upper and lower bounds on the vacuum emission from multi-dimensional surfaces. <sup>11</sup>
C. The results of this approximate method are forced to agree with the exact bulk PCC deep in the material.	This modifies the method into a technique for extrapolating the known bulk currents out to the vacuum interface and minimizes the effect of simplifications D, E and F.
D. The electron angular distribution is expanded in a Legendre polynomial series which is truncated at the $\ell = 1$ term ( $P_1$ approximation) or the $\ell = 2$ term ( $P_2$ approximation).	The effects of multiple electron scattering and/or fairly isotropic electron sources (photoelectric and Auger) are such as to generate electron distributions that are reasonably represented by truncated expansions. The good agreement between the $P_1$ and the more accurate $P_2$ quantum efficiencies in most cases supports the acceptability of this simplification. <u>The one exception is that the code does not predict reasonable angular distributions for electrons back emitted from low-Z materials at high photon energies where the Compton effect dominates.</u>
E. A simple analytical form is used to describe the electron-nuclear scattering cross section's dependence on electron energy.	The results were found to be insensitive to the functional form of the cross section as long as simplification C is used.
F. A constant "average" nuclear scattering cross section is used to describe the transport between the electron's initial energy and its energy on leaving the surface.	The nuclear scattering cross section varies strongly with the electron's energy. This dependence is partially compensated for by using a different constant "average" cross section for each energy at which the emission is observed. The ultimate justification for simplifications D-F is the good agreement between these predictions, detailed Monte Carlo calculations and available experimental data as shown in Reference 2.
G. For non-normally incident plane wave photon fluxes the angular distribution with respect to the surface normal is the average value integrated over all azimuthal angles.	For non-normal incidence the angular distributions are not azimuthally symmetric about the surface normal. These non-normal distributions are valid if the photon source or electron detector has azimuthal symmetry.
H. The electron range is proportional to the energy raised to a power.	This is used only in the calculation of the surface energy deposition. It is an accurate functional form for the range-energy dependence over any limited interval.

Weymouth considers the azimuthally symmetric one-dimensional Boltzmann transport equation in the continuous-slowing-down-approximation. In this approximation, for a monoenergetic source,  $E_0$ , there is a one-to-one correspondence between the path length traversed,  $s$ , and its energy  $E < E_0$ . The path length that an electron will traverse in coming to rest is called its residual range. Primary electrons only are considered. (A later section describes how low energy secondary emission from metallic surfaces is calculated from a knowledge of the surface energy deposition at the vacuum interface.) Weymouth's solution for the vacuum emission currents uses the following procedure:

1. The primary electron distribution function  $F(x, E, \mu = \cos \theta)$  is expanded in a Legendre series which it is assumed can be truncated after  $n + 1$  terms (the  $P_n$  approximation);
2. This allows the Boltzmann integral equation to be converted into a set of  $n + 1$  coupled partial differential equations among the expansion coefficients. The electron elastic scattering cross section enters these equations only through the scattering functions.

$$\kappa_n(E) = \int_{-1}^{+1} \sigma(\mu, E) [1 - P_n(\mu)] d\mu \quad (2)$$

where  $P_n$  is the  $n^{\text{th}}$  Legendre polynomial. The ratios  $\kappa_n/\kappa_1$  are well represented by constants.

3. It is now assumed further that the scattering cross section and, therefore, the scattering functions are independent of energy;
4. This allows Laplace transformation in the variables  $x$  and  $E$ , converting the partial differential equations to coupled algebraic equations which are then solved;
5. The inverse transform in  $x$  is done analytically. At this point, one has algebraic expressions for the transform in energy of the expansion coefficients of the electron distribution function;



6. Finally, the inverse transform in energy is done numerically yielding the vacuum emission current in terms of a number of parameters. These are the constant scattering function  $\kappa_1$  and the Legendre coefficients,  $A_n$ , which describe the initial angular distribution of the anisotropic monoenergetic electron source. Step 6, the inverse transform in energy, is the most difficult part of the solution procedure. Weymouth's procedure is tractable in the  $P_n$  approximation only for very small  $n$ .

Our first significant modification is to introduce energy dependence into the elastic scattering function,  $\kappa_n$ . For electrons created with energy  $E_0$  and emitted into vacuum at an energy  $E < E_0$ , the Laplace transform method requires the use of a constant scattering function over the interval  $(E_0, E)$ . Weymouth used the same constant scattering function for all  $E$ . This is a gross approximation since, in fact, the  $\kappa_n$  vary with energy roughly as the reciprocal of the residual range. In our calculations, we chose a different constant  $\kappa_n$  over the interval  $(E_0, E)$  for each  $E$ . The constants used are certain average values over the interval  $(E_0, E)$  chosen in such a way that far from the interface this transform method reproduces the exact Goudsmit-Saunderson result for the electron energy and angular distribution in the bulk. Use of energy-dependent cross sections amounts to solving a different problem for each  $E$  value of interest. Such a procedure seems at first sight cumbersome, but it is not. Indeed, it is the source of great computational simplification as shown below. To determine average values for the scattering functions, we use the particular functional form

$$\kappa_1(E) = \kappa_1(E_0)s(E_0)/s(E) \quad (7)$$

in which  $s(E)$  is the residual range at energy  $E$ . Calculations performed using a highly accurate functional form of  $\kappa_1$  due to Spencer<sup>12</sup> do not differ significantly from the results obtained using this representation of the energy dependence. With this particular functional form, the number and angular distribution of the emitted electrons can be much more easily determined than in Weymouth's method. This results because integration over the emission energy of the distribution function of electrons obtained in Step 6 of Weymouth's method now takes the form of a Laplace transform in energy. These

transforms are given by the algebraic formulae in Step 5 of Weymouth's method. Therefore, not only have we introduced energy dependence into the scattering cross section, but in so doing we find that we can express the total emission current and angular distribution of the emitted electrons without having to do the inverse transform in energy. In addition, the energy deposition in the material at the vacuum interface can also be calculated without having to do the inverse transform in energy. This is the source of the algebraic formulae presented below. Determination of the energy distribution of emission electrons still requires numerical evaluation of the inverse transform. For convenience, the results of these evaluations have been fit to analytical functions.

Our second significant improvement on Weymouth's method consists in expressing vacuum emission in terms of the bulk quantities considered in the previous section. In Weymouth's method, the monoenergetic electron source is described in the  $P_n$  approximation by only the first  $n + 1$  Legendre polynomial expansion coefficients of the initial electron angular distribution,  $A_n$ . With these sources and the simplifications introduced in Table II, Weymouth's method can be used to calculate bulk PCC. These bulk PCC will not, in general, agree with the accurate bulk PCC produced by the true source as given in Eq. (4). In our method we choose the  $A_n$  so as to require that certain electron current components in the bulk agree exactly with the predictions of the previous section. Similarly, the scattering parameter  $\kappa_1(E_0)$  can be chosen so as to reproduce exactly the known quantity  $R_1(E_0)$ , which is the mean penetration of a monoenergetic electron in an infinite medium along its initial direction. In this form, our method may be thought of as a technique to extrapolate known exact results in the bulk out to the vacuum interface. With this procedure, we find good agreement with experimental data for  $n$  as small as one or two; discrepancies are noted only for back emission and then only for large photon energies and low- $Z$  materials; i.e., for highly anisotropic sources and small scattering. It is in precisely this region that back emission is very small and of little practical consequence.

So far, only monoenergetic electron sources have been discussed in this section. Distributed energy sources of electrons generated by the various photon interactions may be modeled by a superposition of solutions. However, we find that the magnitude and angular distribution of vacuum emission can be well modeled by a single average monoenergetic electron source as long as the coefficients describing the source are constrained to agree with the corresponding bulk currents produced by the photon energy of interest. This is not generally true for the energy distribution, of course.

### B.1. Quantum Efficiency

The quantum efficiency is the total number of electrons emitted into a vacuum per incident photon. For normally incident photons, the formulae for the forward [backward] quantum efficiencies,  $J_{FV}$  [ $J_{BV}$ ], in units of electrons per photon (or [electrons  $\text{cm}^{-2} \text{sec}^{-1}$ ]/[photon  $\text{cm}^{-2} \text{sec}^{-1}$ ]) are

$P_1$  approximation:

$$J_{FV}^1 \left[ J_{BV}^1 \right] = \frac{2(J_F + J_B) + [-] J_N (3/\bar{R}(\bar{E}))^{1/2}}{2 + (3/\bar{R}(\bar{E}))^{1/2}} \quad (8)$$

$P_2$  approximation:

$$J_{FV}^2 \left[ J_{BV}^2 \right] = \frac{t}{W} \left\{ 4Au + [-] 6B \frac{ut(5t + 2u)}{y(4t + u)} + 25Ct \right\} \quad (9)$$

where

$$A = \left\{ J_F + J_B + 4J_F(90) \right\} / 3$$

$$B = J_N / 2\bar{R}(\bar{E})$$

$$C = \left\{ J_F + J_B - 2J_F(90) \right\} \frac{8(t + \alpha)}{15t}$$

$$u = 5(t + \alpha)$$

$$W = 2uy + t(4u + 5y)$$

$$t = \bar{R}(\bar{E}) / [1 - \bar{R}(\bar{E})]$$

$$y = \left\{ 3u(t^2 + t) / (4t + u) \right\}^{1/2}$$

$$\alpha = \kappa_2 / \kappa_1 \approx 2.5$$

$$\bar{R}(\bar{E}) = R_1(\bar{E}) / s(\bar{E})$$

and where  $J_F$ ,  $J_B$  and  $J_N$  are the forward, backward and net bulk PC currents evaluated in the direction of the outward surface normal,  $J_F(90)$  is the

"forward" (= "backward") bulk PC current evaluated perpendicular to the surface normal,  $\bar{E}$  is the average initial electron energy, all evaluated at the photon energy of interest and  $\bar{R}(\bar{E})$  is the mean penetration of electrons of energy  $\bar{E}$  along their initial direction in the bulk expressed in units of their total range. All of these quantities are tabulated in Reference 4. The  $P_1$  formulae (8) should be used except for back emission at high photon energies where the  $P_2$  formulae (9) are better. Where the  $P_2$  result is very different from the  $P_1$  result both are, of course, suspect; this only happens when the quantum efficiency is so low as to be generally of little practical interest.

The formulae for the quantum efficiencies for photons incident at an angle  $\theta_0$  with respect to the outward surface normal are the same except that the currents  $J_N$ ,  $J_F$  and  $J_B$  along the surface normal and  $J_F(90)$  perpendicular to the surface normal are evaluated for photons traveling in the bulk at an angle  $\theta_0$  with respect to the surface normal (but see following paragraph). Note that these formulae for non-normal incidence apply to the prediction of the emitted electron current density in case of a plane wave of photons incident on a finite slab such that as the slab is tilted the number and areal density of photons hitting the slab decreases as  $\cos\theta_0$ . In some practical applications the photon beam is narrower than the target, and as the target is tilted with respect to the photon beam the total number of photons hitting the target is constant. In this latter case, to predict the total number of electrons emitted from the target formulae (1) and (2) should additionally be multiplied by  $\sec\theta_0$ . Finally, to predict the results for a photon spectrum, the formulae must be convolved with the appropriate photon distribution.

In the definition of  $\alpha$  following Eq. (9), the number 2.5 is an approximation of the ratio  $\kappa_2/\kappa_1$ . QUICKE2 actually evaluates this ratio using internal data, but one may use Eq. (9) without access to QUICKE2 by taking this ratio from a table in Reference 4 or simply by using the number 2.5, with very little error. Similarly, when the photon angle of incidence,  $\theta_0$ , is not zero, QUICKE2 evaluates the current components  $J_F$ , etc., exactly. Equations (8) and (9) may be used without access to QUICKE2, however, with very little error, by taking the current components from Reference 4 and using the following procedure: In Eq. (8) multiply  $J_N$  by  $\cos\theta_0$ ; in Eq. (9) multiply coefficients A, B, C by 1,  $\cos\theta_0$ ,  $(3\cos^2\theta_0 - 1)/2$ , respectively.

## B.2. Angular Distribution

The angular distribution in the  $P_1$  approximation is determined entirely by the mathematical formalism; it contains no physics and is only qualitatively correct. For normally incident photons, the  $P_2$  approximation formula for the angular distribution integrated over all energies (electrons/photon/steradian) is

$$\frac{dN}{d\Omega} = \frac{J_{FV}^2}{4\pi} |\mu| \left\{ D + 3|\mu| + 5F \frac{3\mu^2 - 1}{2} \right\} \quad (10)$$

where  $\mu$  is the cosine of the emission angle with respect to the outward surface normal and where

$$F = \frac{4(-2A + 5C)/J_{FV}^2 + 8}{15 + 10\alpha/t} \quad (11)$$

$$D = 2 - 1.25F .$$

The formula for the back angular distribution with respect to the outward normal at the back surface is the same except  $J_{FV}^2$  is replaced by  $J_{BV}^2$  in Eq. (10) and in the definition of  $F$ . For non-normal incidence, the azimuthal symmetry of the angular distribution is lost and our method cannot predict the full angular dependence. However, if either the photon source or electron detector has azimuthal symmetry, then the angular distributions due to photons incidence at an angle  $\theta_0$  with respect to the normal are given by Eq. (10) except that  $J_N$ ,  $J_F$ ,  $J_B$  and  $J_F(90)$  are evaluated for photons traveling at an angle  $\theta_0$  with the surface normal. Again, to use Eq. (10) without access to QUICK2 one may use the procedure described immediately above.

The angular distributions for photoelectric and Auger sources are in good agreement with experimental and Monte Carlo results. For Compton electrons the distributions are not as peaked in the forward direction as the experimental and Monte Carlo results, particularly in materials of lower atomic number. This results from the fact that the Compton electrons are initially strongly forward peaked and are not well represented by the  $P_2$  approximation. The situation is much worse in the backward direction. Our analytical results, although giving reasonable quantum efficiencies, may predict a negative angular distribution near the surface in lower atomic

number materials at high photon energies. This results from the fact that the  $P_2$  approximation to the initial angular distribution of the forward peaked Compton electrons goes negative in the back direction, and there is too little scattering to wipe out this anomaly before it reaches the surface. To get meaningful results, it would be necessary to use a  $P_N$  approximation with  $N > 2$ ; this has not been done at present. Fortunately, at high photon energies the magnitude of back relative to forward emission is small and, therefore, back emission is generally not important in practical problems. We are unaware of any measured high energy back angular distributions. We have found from experience with Monte Carlo calculations, however, that a  $\cos\theta$  dependence is a reasonable approximation to use in this case. When QUICKE2 senses the anomaly just described, a warning statement is printed and a  $\cos\theta$  distribution is substituted.

### B.3. Energy Distribution

The forward  $P_1$  energy distribution (electron/photon/MeV) integrated over angles for a monoenergetic electron source is given by

$$\frac{dN}{dE} = \frac{(J'_F + J'_B) g(q) + J'_N h(q)/\bar{R}(E_0)}{s(E_0) (dE/dx)} \quad (12)$$

where  $E_0$  is the initial electron energy,  $dE/dx$  (MeV cm<sup>2</sup>/gm) is the stopping power at energy  $E$ ,  $s(E)$  (gm/cm<sup>2</sup>) is the residual range of electrons of energy  $E$ ,  $J'_F$ ,  $J'_B$  and  $J'_N$  are the contributions to the bulk PC currents produced by this monoenergetic source and

$$q = t^{-1} \ln \left[ s(E_0)/s(E) \right]$$

$$g(q) = (23.94 + 3\pi q/4)^{-1/2} + (2.088 + .5107q)^{-3/2} \quad (13)$$

$$h(q) = (21.99 + (3\pi)^{1/3} q)^{-3/2} + (1.848 + .5373a)^{-5/2}$$

$$+ .2391 \exp(-.7865q) \quad (14)$$

The formulae for back emission are the same except that the sign of  $J'_N$  is changed. To get accurate results, one must sum results separately over the various energies of the electron source (Compton, photoelectric and Auger) and we do this superposition by computer. Note that in the  $P_1$  approximation the energy spectrum is the same at all emission angles.

#### B.4. Surface Energy Deposition and Low Energy Secondary Electrons

Calculation of the energy deposition in the material at the vacuum interface is important because empirically it has been found that for many metals the magnitude of emission of very low-energy (<50 eV) secondary electrons is proportional to the surface dose.<sup>13</sup> To calculate the deposition it is necessary to introduce the further simplification that the range of electrons in the material  $s(E)$  is proportional to the energy raised to a power.

$$s(E) \propto E^m \quad (13)$$

The constant  $m$  is defined in practice by

$$m \equiv \ln [s(\bar{E})/s(\bar{E}/2)]/\ln 2 \quad (14)$$

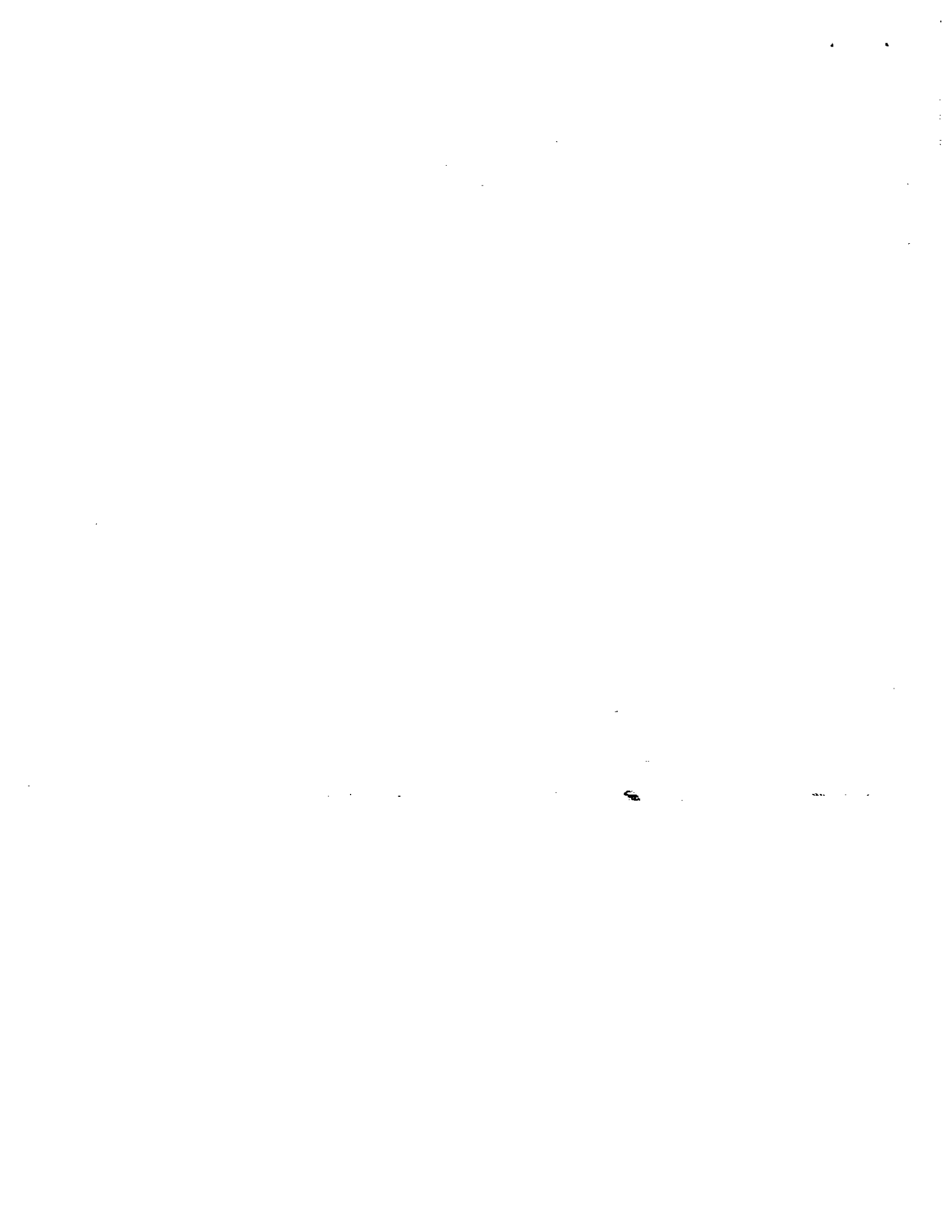
The formulae for the energy deposition at the fore [back] surface in units of (MeV/gm)/(photon/cm<sup>2</sup>) are

$$P_1 \text{ approximation} \\ D_F^1 [D_B^1] = \frac{2\sigma_{en} h\nu}{2+\sqrt{3}(1+1/t^*)} \left\{ 1 + [-] \frac{J_N \sqrt{3/(1+1/t^*)}}{2\bar{R}(\bar{E}) (J_F + J_B)} \right\} \quad (15)$$

$$P_2 \text{ approximation} \\ D_F^2 [D_B^2] = \frac{\sigma_{en} h\nu t^*}{AW} \left\{ A(4u + 5y) - [+ ] \frac{12u^2 t^*}{4t^* + u} \frac{B}{y} - 12.5Yc \right\} \quad (16)$$

where  $\sigma_{en}$  [cm<sup>2</sup>/gm] is the photon energy absorption cross section evaluated at the photon energy,  $h\nu$  [MeV], of interest. In these equations  $t^* \equiv t/m$  and the quantities  $u$ ,  $y$ ,  $W$  are to be evaluated using  $t^*$  rather than  $t$ , but the source terms  $A$ ,  $B$ ,  $C$  and the current components are as previously defined. For non-normal photons  $J_N$ ,  $J_F$ ,  $J_B$  and  $J_F(90)$  are evaluated for photons traveling at an angle  $\theta_0$  with respect to the normal as discussed above.

The deposition at the back surface of a low  $Z$  material exposed to high energy photons is not accurately calculated in the  $P_2$  approximation. The source of the error is the same as in the angular distribution calculation. When the  $P_2$  results are significantly different from the  $P_1$  results both are suspect. If the  $P_2$  energy deposition goes negative, an error message is printed out.





#### IV. Computational Details

The purpose of this section is to provide a summary of the details and organization of the program. Additional information is given in Appendix I where the material data are discussed. All subroutines and functions described below are called from QUICKE2 unless otherwise noted.

##### Program QUICKE2

This is the main subroutine. The input cards are read in (see Appendix II) and the input information is printed out. Subroutine PREP is called to prepare the cross sectional information. The PCC are calculated for each monochromatic photon energy sequentially. First, the Compton electrons are treated. The continuous set of Compton electron energies and angles is treated as a finite set of monoenergetic, monodirectional electrons weighted according to the Klein-Nishina cross section. The total Compton response is given by the sum of the responses for each individual source. Next photoelectric processes are treated. A DO loop calculates the photoelectric response for each element in the material. The photon energy is tested to see if it is above the K, average L, average M or average N shell energy. If the energy is above the average L shell, then the contribution of Auger electrons to forward (= back) current and emission energy distribution is computed. Then the contributions from the photoelectric electrons emitted from each allowed shell are considered. The photoelectric response is the sum of the responses from all the shells of all the elements in the material. For any individual electron source its net bulk PCC is calculated and subroutine FORCUR is called twice to determine the forward bulk PCC along the reference direction and perpendicular to the reference direction. If vacuum emission energy distributions are desired then the emission spectra due to each individual source is evaluated. Two average initial electron energies are calculated, one weighted by the contribution of each source energy to the net current and one calculated by weighting each source energy by the contribution to the forward plus backward currents. Once the bulk currents

for the photon energy are known, then the  $P_1$  and  $P_2$  quantum efficiencies and surface energy depositions are calculated. All the above results are then printed out. Then the angular distribution and energy distributions of emission electrons are calculated and printed out. After all the monoenergetic photon responses are calculated the response to the input photon spectrum, if any, is found by trapezoidal integration.

#### Subroutine PREP

This subroutine reads in the material data from the data bank as described in Appendix I. Subroutine RANGE is called to calculate the range from the stopping power. The  $R_N$  are then calculated according to Eq. (6) at a predetermined finite set of energies.

#### Function TRBARF(EE)

This subroutine returns the value of  $R_1/R_0$  (Eq. 6) which is the mean penetration of an electron of energy EE along its initial direction divided by its total pathlength (csda range).

#### Subroutine PICON

Evaluates the functions that are needed to determine the emission spectra (Eqs. 13 and 14).

#### Subroutine VCON

Determines the ratio of  $\kappa_2/\kappa_1$  which is needed in the  $P_2$  approximation.

#### Function DEDXFN(E)

Determines the stopping power at energy E by linear interpolation.

#### Function PELEC(K,HV)

Determines the ratio of the net current calculated with PELEC angular distributions to the current calculated with the Fischer/Sauter formulae for the  $K^{\text{th}}$  element in the material at a photon energy HV. Linear interpolation is used.

### Function RBARFN(EE)

Returns the value of  $R_1$  in units of  $\text{gm/cm}^2$ . Note that  $\text{RBARFN(EE)}/\text{TRBARF(EE)}$  gives the range in  $\text{gm/cm}^2$ . Logarithmic interpolation is used below 1 MeV and linear interpolation is used above 1 MeV.

### Subroutine FORCUR

Calculates the contribution to the bulk forward current along the reference direction and perpendicular to the reference direction for an individual electron source with range  $S_0$  as given by Eq. (4). The value of  $R_N$  at  $S_0$  is found by interpolation. For Compton electrons this source has a unique direction. For photoelectric interactions this monoenergetic source is distributed in angle. Subroutine INT is called to determine the Legendre polynomial expansion coefficients of the photoelectric angular distribution. For Auger electrons the source is isotropic.

### Function FORCOS(EE,HV)

Calculates the average cosine of the Fischer or Sauter photoelectric angular distribution in the forward half plane for photoelectrons of energy EE created by photons of energy HV. Called from FORCUR.

### Subroutine INT

Calculates the Legendre polynomial expansion coefficients for the Fischer or Sauter distribution. Called from FORCUR.

### Subroutine COEF

Calculates values for INT. Called from INT.

### Subroutine AVCOS

Calculates the average cosine for photoelectrons for the Fischer or Sauter distribution. Used in calculating the net PCC for photoelectric electrons.

### Subroutine CRSEC

Evaluates the Biggs photoelectric interaction cross section.

Subroutine RANGE

Calculates the range from the stopping power. Very similar to SANDYL range routine. Called from PREP.

Subroutine ZINT

Numerical integration routine. Called from RANGE.

APPENDIX I  
MATERIAL DATA

The calculations require material data relevant to photon and electron transport, most of which is stored in a data bank on a tape or in permanent files, and the remainder is calculated in the code from the corresponding formulae.

The data bank has 25 files, one for each element. Subroutine PREP reads the information from the file for each element in the material being irradiated. A composite atomic weight, stopping power, scattering parameter and photon cross section are calculated by weighting each element by its weight fraction. The stopping power and electron-nuclear scattering parameters are taken from the SANDYL code. For each element the data are arranged as follows:

A. ZN, ATWTN, NN, ELEM

FORMAT (F10.1, F10.4, I10, A10)

AN - atomic number

ATWTN - atomic weight

NN - file number

ELEM - alphanumeric element name

B. JL, TEDZ (TEDSBE(J),J=1,9)

FORMAT (I3, F5.2, 9F8.3)

JL - number of sets of Biggs photoelectric cross section parameters

TEDZ - atomic number (same as ZN)

TEDSBE - energy of K, L1, L2, L3, M1, M2, M3, M4, M5 levels in MeV

C. (FINISH(J), (A(J,L),L=1,4),J=1,JL)

FORMAT (10X, F12.3, 4E11.3)

FINISH - maximum energy in MeV of the  $J^{\text{th}}$  set of photoelectric cross section parameters

A - four parameters - if the photon energy  $h\nu$  is  $\text{FINISH}(J-1) < h\nu < \text{FINISH}(J)$  then ( $\text{FINISH}(0) = 0$ ,  $\text{FINISH}(JL+1) = \infty$ ).

$$\sigma_{\text{PE}} = \sum_{L=1}^4 A(J,L)/E^{**L}$$

D. (ZSAN,ESAN(J),RSAN(J),SSAN(J),ESAN(J+1),RSAN(J+1),SSAN(J+1),J=1,64,2)

FORMAT (F5.1, 6E12.5)

ZSAN - atomic number (same as ZN)

ESAN - set of 64 energies in MeV at which the electron-nuclear cross sectional information is stored.

RSAN - range of electron in  $\text{gm/cm}^2$  with energy ESAN from SANDYL.

SSAN -  $K_1$  of Equation (2) times the range RSAN evaluated at ESAN from SANDYL.

E. ST(1,J) (TEBL(K,J),K=1,9)

FORMAT (3X, 7E11.4) - called 64 times

ST(1,J) - energy in units of .51 MeV

TEBL(K,J) - the inverse of the stopping power in units of  $(\text{MeV/gm/cm}^2)^{-1}$  evaluated at equal intervals between ST(1,J) and ST(1,J+2). K=1 corresponds to energy ST(1,J). K=N corresponds to energy ST(1,J) -  $\frac{N}{10} (\text{ST}(1,J) - \text{ST}(1,J+1))$ . Data from SANDYL.

F. LMAX(J),TEDZ,ESAN(J),RSAN(J)

FORMAT (I10, F10.2, 2E20.10) - F. and G. called 64 times.

LMAX - number of  $K_N$  (Eq. 2) for ESAN(J)

TEDZ - atomic number

ESAN, RSAN - same as Card 4.

G. (SSAN(M),M=2,LMAX)

FORMAT (3X, 7E11.4)

SSAN -  $K_n$ ,  $n=2$ , LMAX. Data from SANDYL.

H. (RATIO(J),J=1,24)

FORMAT (6E20.10)

RATIO - ratio between the net current calculated with the photoelectric angular distributions from the PELEC code to the net currents calculated with the Fischer/Sauter formulae evaluated at .01, .015, .02, .03, .04, .05, .06, .07, .08, .09, .10, .125, .15, .2, .3, .4, .6, .8, 1., 2., 4., 7., 10. and 20. MeV respectively.

Photoelectrons can be generated in the code from the K level or any average L, M or N level. A photoelectric interaction can eject an electron from any shell whose binding energy is less than the photon energy. The relative probabilities of the interaction from each shell are calculated as follows. Just below the K edge the photon interacts with only the lower shells. Just above the K edge energy the cross section jumps because of the K shell interactions while the interaction due to lower shells remains constant. Just above the K edge the ratio of the number of K shell interactions to all other shell interactions is

$$\frac{\sigma_{PE}(E_K + \delta) - \sigma_{PE}(E_K - \delta)}{\sigma_{PE}(E_K + \delta)}$$

We assume that this ratio holds for all energies above the K edge. Similarly, the jump in the cross section at the L edge determines the ratio of L shell interactions to all lower shell interactions. Again, we assume that this ratio holds for all energies above the L edge. In this manner the relative probabilities are determined.

The probability that a K shell ionization results in an Auger electron of energy  $E_K - 2E_{L2}$  is taken as

$$ZCON = \frac{1.}{1. + (Z/30.)^4}$$

The probability that a K shell ionization results in an Auger electron of energy  $E_{L2} - 2E_{M3}$  is taken as

$$ZCONKL = \frac{1.}{1. + (Z/81)^4} + \frac{.65}{1. + (Z/30)^6}$$

The probability that a L shell ionization results in an Auger electron of energy  $E_{L2} - 2E_{M3}$  is taken as

$$ZCONL = \frac{1.}{1. + (Z/92)^4}$$

The energy absorption cross section for Compton interactions is taken from Biggs analytical approximation to the Klein Nishina cross section

$$\sigma_{ea}^{KN} = .4006 \frac{X + .825X^2 + .93234X^3}{1 + 5.393X + 5.212X^2 + .8783X^3 + .01599X^4} \frac{Z}{A}$$

where

$$X = \frac{E(\text{MeV})}{.511}$$

The energy absorption cross section for photoelectric interactions is related to the interaction cross section by

$$\sigma_{en}^{PE} = \sigma_i^{PE} \frac{h\nu - E_{LOST}}{h\nu}$$

where  $h\nu$  is the photon energy and  $E_{LOST}$  is the energy of the fluorescent radiation. The probability that the K or L shell will fluoresce is just one minus the probability that it will emit an Auger electron which is given above. The average K and L shell fluorescent energies were taken from Storm and Israel.<sup>14</sup>

For metals the yield of very low energy secondary electrons is found empirically to be proportional to the energy deposition at the surface. The proportionality constants used were taken from Reference 13 and are given in Table III.



TABLE III

EMPIRICAL RATIO OF SECONDARY ELECTRON  
YIELD TO SURFACE DEPOSITION

METAL	ATOMIC NUMBER	RATIO* [e <sup>-</sup> /cm <sup>2</sup> ]/[MeV/gm]
Al	13	.017
Ti	22	.014
Ni	28	.017
Cu	29	.017
Ag	47	.022
Sn	50	.016
Ta	73	.025
Au	79	.023
Pb	82	.024

\*From E. A. Burke, et al., IEEE Trans. Nucl. Sci., NS-17, 193 (1970).

The first part of the document discusses the importance of maintaining accurate records of all transactions. It emphasizes that every entry, no matter how small, should be recorded to ensure the integrity of the financial statements. This includes not only sales and purchases but also expenses and income.

The second part of the document provides a detailed breakdown of the company's assets and liabilities. It lists the various types of assets, such as cash, accounts receivable, and inventory, and provides a clear explanation of how each is valued. Similarly, it details the company's liabilities, including accounts payable and long-term debt, and explains the methods used to measure their impact on the balance sheet.

The third part of the document focuses on the company's income statement. It shows how the company's revenue is calculated and how various expenses are deducted to arrive at the net income. This section also discusses the company's operating costs and provides a clear picture of its profitability over the reporting period.

Finally, the document concludes with a summary of the company's overall financial performance. It highlights the key findings from the financial statements and provides a clear picture of the company's financial health. This includes a discussion of the company's liquidity, solvency, and overall financial stability.

APPENDIX II  
INPUT CARDS

This appendix describes the input cards necessary to run a problem with QUICKE2. Several problems may be run sequentially. The user has the option of using or redefining a set of default values for many of the input variables which will be used in all subsequent problems in a given computer run unless redefined.

Card	Columns	Variable	Description
1	1-80	HEAD	80 Character alpha-numeric problem title
2	1-5	NUMEL	Number of elements in the material > 0 Number of elements to be read in on Card 3 (new material or first problem) = 0 Program terminates < 0 Same material as previous problem. - 1 x NUMEL is the number of elements. Card 3 is omitted (may not be used in the first problem).
	6-10	NPCT	= 0 Atomic or chemical fraction used to describe material on Card 3 (e.g., water = .667 H, .333 O) = 1 Weight fractions (e.g., water = $\frac{2}{18}$ H, $\frac{16}{18}$ O)
	11-15	NHVCALC	Number of photon energies at which currents are calculated. = 0 will use values from previous problem; if this is the first problem the 24 photon energies used are .01, .015, .02, .03, .04,

Card	Columns	Variable	Description
			.05, .06, .08, .10, .15, .2, .3, .4, .5, .6, .8, 1., 1.3, 2., 3., 4., 5., 6., 10. MeV. > 0 These values in MeV must be read in on Card 4 and will be used in subsequent problems unless redefined. Maximum number 50.
16-20		NTYPE	= 0 Bulk currents and magnitude and angular distribution of emission currents calculated. = 1 Bulk currents only.
21-25		NDNDE	Applicable only if NTYPE = 0 = 0 Emission energy distribution calculated. = 1 No emission energy distribution calculated.
26-30		NSPECT	Number of spectrum points = 0 If this is the first problem no spectrum response is desired; otherwise, the spectrum (or no spectrum) from previous problem will be used. > 0 Read in on Card 6 NSPECT values of a number vs. energy photon spectrum (dN/dE). < 0 Read in on Card(s) 7 NSPECT  values of an energy vs. energy spectrum (dE/dE).
31-35		NECALC	Number of energies at which emission energy spectrum will be calculated if NTYPE = 0 and NDNDE = 0. = 0 Use values from previous problem. If this is the first problem the 34 values in MeV are .001, .003, .005, .007, .010, .015, .020, .030, .040, .050, .060, .070, .080, .090, .10, .15, .20, .30, .40, .50, .60, .70, .80, 1.0, 1.5, 2.0, 3.0, 4.0, 5.0, 6.0, 7.0, 8.0, 10. > 1 Read in on card(s) 5 NECALC values (maximum 34)

Card	Columns	Variable	Description
	36-40	NHVANG	= 0 Use photon angle from the previous problem. If this is the first problem the photon angle will be 0 degrees. = 1 Read in new photon angle on Card 6.
	41-45	IPRINT	= 0 Does not print cross sections from input tape. = 1 Will print cross sections from input tape.

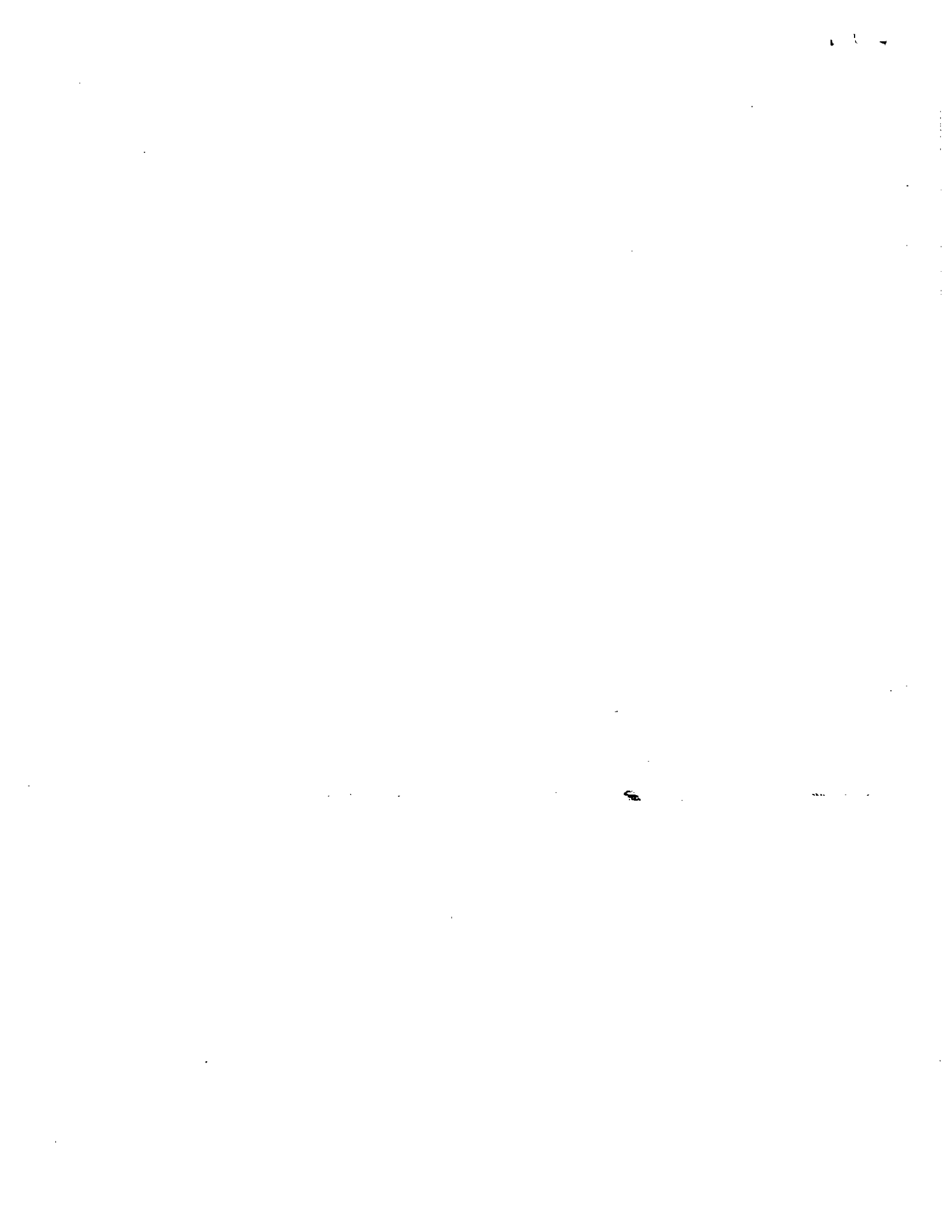
3

(Required if NUMEL >0, Card 2, Cols. 1-5)  
 NEL(I),  
 F(I)  
 NUMEL pairs of values of atomic numbers, NEL(I), and element fractions, F(I), which are chemical fractions if NPCT = 0 or weight fractions of NPCT = 1 (Card 2, Cols. 6-10). The atomic numbers are chosen from

<u>Z</u>	<u>Name</u>
1	Hydrogen
4	Beryllium
6	Carbon
7	Nitrogen
8	Oxygen
9	Fluoride
12	Magnesium
13	Aluminum
14	Silicon
17	Chlorine
18	Argon
20	Calcium
22	Titanium
26	Iron
28	Nickel
29	Copper
32	Germanium
41	Niobium

Card	Columns	Variable	Description
			47 Silver
			50 Tin
			60 Neodymium
			73 Tantalum
			79 Gold
			82 Lead
			92 Uranium
	1-2		Z of first material, Format I2
	8-10		F(1), Format F8.6
	11-12		Z of second material
	13-20		F(2)
	21-22		Z of third material
	23-30		F(3); etc., up to NEL(NUMEL), F(NUMEL)
4	8F10.7	HVCALC	<p><u>(Required if NHVCALC &gt;0, Card 2, Cols. 11-15)</u>  NHVCALC values of the photon energies at which these currents are to be calculated are read in eight to a card. The photon energies in MeV should be in ascending order. Minimum .001 MeV; maximum 10 MeV. If a spectrum is to be used, the minimum photon energy should be less than or equal to the minimum spectrum energy and the maximum photon energy should be greater than or equal to the maximum spectrum energy.</p>
5	8F10.7	ECALC	<p>(Required if NECALC &gt;1, Card 2, Cols. 31-35)  NECALC values of the energies at which the electron emission energy distribution are to be calculated are read in eight to a card. The</p>

Card	Columns	Variable	Description
			energies in MeV should be in ascending order. Minimum .001 MeV, maximum = maximum photon energy.
6	F10.7	HVDEG	<p><u>(Required if NHVANG &gt;1, Card 2, Cols. 36-40)</u> For vacuum emission: photon angle of incidence in degrees, for bulk currents: the angle relative to the photon direction at which the currents are calculated.</p>
7	8F10.7	DNDESP, HVSPECT	<p><u>(Required if NSPECT ≠ 0, Card 2, Cols. 26-30)</u> NSPECT pairs of spectrum intensity and energy (in MeV) are read in four pairs to a card. The energy values must be in ascending order. The spectrum need not be normalized.</p> <p><u>If another problem follows, go to Card 1. Otherwise, two additional blank cards are required to normally terminate the program.</u></p>





## APPENDIX III OUTPUT INFORMATION

The output of QUICKE2 is extensively annotated to allow easy user interpolation of the results. An outline of the output is given below.

### Always Printed

#### A. Input Information

1. Problem title
2. Number, names and fractions of elements
3. Type of problem - bulk or vacuum
4. Number of energies of monoenergetic photons and values in MeV at which the response is calculated.
5. Photon angle of incidence.

#### Only if vacuum emission energy distributions are to be calculated

6. Number of energies at which emission spectra are calculated and values in MeV.

#### Only if response to photon spectrum is to be calculated

7. Input photon spectrum and equivalent monoenergetic photon source weighted according to the input spectrum.

### Only Printed if Cross Sectional Information is Desired

#### B. Cross Sectional Information

1. For each element in the material
  - a. Element number, atomic number, atomic weight and name
  - b. Fraction of photoelectric events that Auger
  - c. Photoelectric absorption edge energies
  - d. Parameters for Bigg's photoelectric cross section
  - e. Ratios of the photoelectric cross section from each shell to the total photoelectric cross section.

- f. Ratio of PELEC/Fischer-Sauter net currents
2. Composite expansion coefficients,  $\kappa_n$ , of electron nuclear scattering for the material.
3. Energy, range, mean range, and stopping power table for material.

Always Printed

C. Response to monoenergetic photons

1. Photon energy and angle of incidence
2. Photon interaction and energy absorption cross sections
3. Bulk currents along direction of surface normal
4. Bulk currents perpendicular to normal directions
5. Mean initial electron energy generated by the photons weighted according to contribution: (1) to the net, or (2) the forward plus back bulk currents.
6. Range of electrons of mean energies and photon energy.
7. Constant  $m$  for range-energy functional form,  $S \propto E^m$

For bulk currents only go to D.

8. Fore and back quantum efficiencies.
9. Energy deposition in the material at vacuum interface. Note: If back energy depositions are not accurate they are omitted and a message is printed.

Only if empirical ratio of low energy emission/surface deposition is known.

10. Empirical ratio and magnitude of low energy emission. Note: If back energy depositions are omitted in C. 9, then no back low energy emission is given.
11. Angular distribution of emitted electrons integrated over all emission energies. Note: If  $P_2$  back angular distribution is not accurate an error message is printed and an approximate cosine distribution is substituted.

Only if emission energy distribution is to be calculated.

12. Emission energy distribution. The integrated totals give the quantum efficiency calculated for the true electron source and can be compared to C.8 which is calculated assuming a monoenergetic source.

Only printed if response to a photon spectrum is to be calculated.

- D. Normalized spectrum response similar to response to monoenergetic photons.

1

APPENDIX IV  
SAMPLE PROBLEM

As an illustrative example, the bulk and vacuum PCC will be calculated for Al exposed to 1.25 MeV photons incident at 30°. The input cards are shown below.

1	2	3	4	5	6	7	8	9	10	11	12	13	14	15	16	17	18	19	20	21	22	23	24	25	26	27	28	29	30	31	32	33	34	35	36	37	38	39	40	41	42	43	44	45	46	47	48	49	50	51	52	53	54	55	56	57	58	59	60	61	62	63	64	65	66	67	68	69	70	71	72	73	74	75	76	77	78	79	80	
QUICKER SAMPLE PROBLEM 1.25 MEV PHOTONS INCIDENT ON AL AT 30 DEG.													(CARD 1)													(CARD 2)													(CARD 3)													(CARD 4)													(CARD 6)															
13	1	1	0																																																																													
30.	1	25																																																																														
(BLANK CARD)													(BLANK CARD)													(BLANK CARD)													(BLANK CARD)													(BLANK CARD)																												
-NOTE: CARDS 5 + 7 NOT REQUIRED FOR THIS PROBLEM -																																																																																
1	2	3	4	5	6	7	8	9	10	11	12	13	14	15	16	17	18	19	20	21	22	23	24	25	26	27	28	29	30	31	32	33	34	35	36	37	38	39	40	41	42	43	44	45	46	47	48	49	50	51	52	53	54	55	56	57	58	59	60	61	62	63	64	65	66	67	68	69	70	71	72	73	74	75	76	77	78	79	80	

QUICK2 SAMPLE PROBLEM 1.25 MEV PHOTONS INCIDENT ON AL AT 30 DEG.  
 NUMBER OF ELEMENTS = 1  
 MATERIAL 1 IS ALUMINUM ELEMENT NO. 8 ATOMIC FRACTIONS.000000

NTYPE = 0 VACUUM PHOTOEMISSION - QUANTUM EFFICIENCY AND ANGULAR DISTRIBUTION  
 - ENERGY DISTRIBUTION  
 THE NO. OF PHOTON ENERGIES, NHYCALC = 1 VALUES IN MEV

1.250E+00  
 THE PHOTON ANGLE WITH THE NORMAL = 30.0 DEGREES  
 THE 33 ELECTRON ENERGIES IN MEV AT WHICH THE EMISSION ENERGY SPECTRUM IS CALCULATED ARE  
 1.000E-03 3.000E-03 5.000E-03 7.000E-03 1.000E-02 1.500E-02 2.000E-02 3.000E-02 4.000E-02 5.000E-02  
 6.000E-02 7.000E-02 8.000E-02 9.000E-02 1.000E-01 1.500E-01 2.000E-01 3.000E-01 4.000E-01 5.000E-01  
 6.000E-01 7.000E-01 8.000E-01 1.000E+00 1.500E+00 2.000E+00 3.000E+00 4.000E+00 5.000E+00 6.000E+00  
 7.000E+00 8.000E+00 1.000E+01

----- PHOTON ENERGY = 1.250 MEV - ANGLE OF INCIDENCE = 30.0 DEGREES -----

PHOTON INTERACTION CROSS SECTIONS - KLEIN NISHINA = .0547 PHOTOELECTRIC = .0000 TOTAL = .0547  
 PHOTON ENERGY ABS. CROSS SECTIONS - KLEIN NISHINA = .0250 PHOTOELECTRIC = .0000 TOTAL = .0250

BULK CURRENTS ALONG THE NORMAL DIRECTION

NET CURRENT= 4.64E-03ELECTRONS/PHOTON  
 CONTRIBUTION FROM COMPTON ELECTRONS = 4.64E-03  
 CONTRIBUTION FROM ALUMINUM PHOTOELECTRONS = 3.85E-06  
 FORE CURRENT= 6.75E-03ELECTRONS/PHOTON  
 CONTRIBUTION FROM COMPTON ELECTRONS = 6.75E-03  
 CONTRIBUTION FROM ALUMINUM PHOTOELECTRONS = 5.50E-06  
 CONTRIBUTION FROM AUGER ELECTRONS = 5.23E-11  
 BACK CURRENT= 2.11E-03ELECTRONS/PHOTON  
 CONTRIBUTION FROM COMPTON ELECTRONS = 2.11E-03  
 CONTRIBUTION FROM ALUMINUM PHOTOELECTRONS = 5.50E-06  
 CONTRIBUTION FROM AUGER ELECTRONS = 5.23E-11

BULK CURRENTS PERPENDICULAR TO THE NORMAL DIRECTION  
 FORE CURRENT= 3.79E-03ELECTRONS/PHOTON  
 BACK CURRENT= 3.79E-03ELECTRONS/PHOTON  
 MEAN INITIAL ELECTRON ENERGY WEIGHTED BY CONTRIBUTION TO THE NET BULK CURRENT, EBAR = .8258MEV  
 MEAN INITIAL ELECTRON ENERGY WEIGHTED BY CONTRIBUTION TO FORE+BACK BULK CURRENT, EBAR2 = .8048MEV  
 RANGE OF .8258 MEV ELECTRON= 4.34E-01(GM/CM2) MEAN PENETRATION/RANGE = .365  
 RANGE OF .8048 MEV ELECTRON= 4.20E-01(GM/CM2) MEAN PENETRATION/RANGE = .364  
 RANGE OF 1.2500 MEV ELECTRON= 7.17E-01(GM/CM2) MEAN PENETRATION/RANGE = .387  
 ANALYTICAL FIT-RANGE=ENERGY\*\*M, M= 1.336

VACUUM EMISSION CURRENTS FOR PHOTONS INCIDENT AT 30.0DEGREES WITH RESPECT TO SURFACE NORMAL

QUANTUM EFFICIENCY IN UNITS OF ELECTRONS/PHOTON  
 FORE - P1 APPROX.= 6.36E-03 P2 APPROX.= 6.36E-03  
 BACK - P1 APPROX.= 9.08E-04 P2 APPROX.= 8.48E-04

ENERGY DEPOSITION AT VACUUM INTERFACE IN UNITS OF (MEV/GM) / (PHOTON/CM2)  
 FORE - P1 APPROX.= 2.10E-02 P2 APPROX.= 2.10E-02  
 BACK - P1 APPROX.= 3.98E-03 P2 APPROX.= 3.25E-03

EMPIRICAL RATIO OF LOW ENERGY SECONDARY ELECTRONS TO SURFACE ENERGY DEPOSITION = .0120ELECTRONS/CM2 / (MEV/GM)

QUANTUM EFFICIENCY FOR VERY LOW ENERGY SECONDARY ELECTRONS IN UNITS OF ELECTRON/PHOTON  
 FORE - P1 APPROX.= 2.52E-04 P2 APPROX.= 2.52E-04  
 BACK - P1 APPROX.= 4.78E-05 P2 APPROX.= 3.98E-05

ANGULAR DISTRIBUTION INTEGRATED OVER ALL EMISSION ENERGIES IN UNITS OF ELECTRONS/PHOTON/STERADIAN AND /DEGREE  
 NONNORMALLY INCIDENT PHOTONS. ELECTRON ANGULAR DISTRIBUTION DOES NOT HAVE AZIMUTHAL SYMMETRY ABOUT SURFACE NORMAL.  
 CALCULATED DISTRIBUTION IS AVERAGED OVER AZIMUTHAL ANGLES. APPROPRIATE WHEN PHOTON SOURCE OR ELECTRON DETECTOR HAS AZIMUTHAL SYMMETRY

EMISSION ANGLES MEASURED WITH RESPECT TO SURFACE NORMAL

EMISSION FROM FORWARD SURFACE		EMISSION FROM BACK SURFACE	
EMISSION ANGLE(DEGS)	DN/D(STERADIAN)	EMISSION ANGLE(DEGS)	DN/D(STERADIAN)
0.0	2.84E-03	0.0	6.25E-10
10.0	2.76E-03	10.0	5.25E-05
20.0	2.51E-03	20.0	9.43E-05
30.0	2.15E-03	30.0	1.18E-04
40.0	1.71E-03	40.0	1.20E-04
50.0	1.24E-03	50.0	1.04E-04
60.0	8.08E-04	60.0	7.67E-05
70.0	4.43E-04	70.0	4.56E-05
80.0	1.71E-04	80.0	1.85E-05
90.0	-9.32E-10	90.0	-1.02E-10
100.0	1.34E-05	100.0	-1.02E-10
110.0	4.40E-05	110.0	1.45E-06
120.0	9.34E-05	120.0	4.53E-06
130.0	1.59E-04	130.0	8.87E-06
140.0	2.35E-04	140.0	1.34E-05
150.0	3.11E-04	150.0	1.66E-05
160.0	3.77E-04	160.0	1.71E-05
170.0	4.21E-04	170.0	1.41E-05
180.0	4.36E-04	180.0	8.01E-06
			0.

EMISSION ELECTRON ENERGY DISTRIBUTION INTEGRATED OVER ALL EMISSION ANGLES IN UNITS OF ELECTRONS/PHOTON/MEV

ELECTRON ENERGY	EMISSION FROM FORWARD SURFACE				EMISSION FROM BACK SURFACE				TOTAL
	COMPTON ELECTRONS	PHOTO ELECTRONS	AUGER ELECTRONS	TOTAL	COMPTON ELECTRONS	PHOTO ELECTRONS	AUGER ELECTRONS	TOTAL	
.001	6.00E-05	2.06E-08	5.11E-08	5.00E-05	5.59E-05	1.90E-08	5.11E-08	5.59E-05	
.003	1.29E-04	4.34E-08	0.	1.29E-04	1.18E-04	3.94E-08	0.	1.18E-04	
.005	1.91E-04	6.47E-08	0.	1.91E-04	1.73E-04	5.61E-08	0.	1.73E-04	
.007	2.54E-04	8.52E-08	0.	2.54E-04	2.28E-04	7.60E-08	0.	2.28E-04	
.010	3.49E-04	1.15E-07	0.	3.49E-04	3.08E-04	1.02E-07	0.	3.09E-04	
.015	4.98E-04	1.64E-07	0.	4.98E-04	4.33E-04	1.43E-07	0.	4.33E-04	
.020	6.55E-04	2.12E-07	0.	6.55E-04	5.56E-04	1.82E-07	0.	5.56E-04	
.030	9.57E-04	3.05E-07	0.	9.57E-04	7.84E-04	2.57E-07	0.	7.84E-04	
.040	1.23E-03	3.95E-07	0.	1.23E-03	9.82E-04	3.27E-07	0.	9.83E-04	
.050	1.52E-03	4.84E-07	0.	1.52E-03	1.18E-03	3.94E-07	0.	1.18E-03	
.060	1.81E-03	5.70E-07	0.	1.81E-03	1.35E-03	4.57E-07	0.	1.35E-03	
.070	2.09E-03	6.55E-07	0.	2.09E-03	1.51E-03	5.17E-07	0.	1.51E-03	
.080	2.37E-03	7.36E-07	0.	2.37E-03	1.65E-03	5.71E-07	0.	1.65E-03	
.090	2.60E-03	8.16E-07	0.	2.60E-03	1.78E-03	6.23E-07	0.	1.78E-03	
.100	2.87E-03	8.99E-07	0.	2.87E-03	1.89E-03	6.74E-07	0.	1.89E-03	
.150	4.09E-03	1.28E-06	0.	4.09E-03	2.26E-03	8.00E-07	0.	2.26E-03	
.200	5.13E-03	1.63E-06	0.	5.13E-03	2.40E-03	1.03E-06	0.	2.40E-03	
.300	6.82E-03	2.30E-06	0.	6.82E-03	2.21E-03	1.19E-06	0.	2.22E-03	
.400	7.91E-03	2.92E-06	0.	7.91E-03	1.71E-03	1.22E-06	0.	1.71E-03	
.500	8.56E-03	3.51E-06	0.	8.56E-03	1.13E-03	1.15E-06	0.	1.13E-03	
.600	8.71E-03	4.10E-06	0.	8.71E-03	5.85E-04	1.02E-06	0.	5.86E-04	
.700	8.32E-03	4.67E-06	0.	8.33E-03	1.68E-04	8.34E-07	0.	1.69E-04	
.800	7.62E-03	5.26E-06	0.	7.42E-03	0.	6.10E-07	0.	6.10E-07	
1.000	2.13E-03	6.41E-06	0.	2.13E-03	0.	7.00E-08	0.	7.00E-08	
INTEGRATED TOTALS	6.37E-03	5.23E-06	4.82E-11	5.37E-03	9.02E-04	7.50E-07	4.82E-11	9.03E-04	



## REFERENCES

1. C. J. MacCallum and T. A. Dellin, J. Appl. Phys., 44 1878 (1973).
2. T. A. Dellin and C. J. MacCallum, IEEE Trans. Nucl. Sci., NS-20 91 (1973).
3. T. A. Dellin and C. J. MacCallum, to be published.
4. T. A. Dellin and C. J. MacCallum, Sandia Laboratories Report SCL-RR-720086 (December 1972).
5. H. M. Colbert, "SANDYL: A Computer Program for Calculating Combined Photon-Electron Transport in Complex Systems," Sandia Laboratories Report SCL-DR-720109 (March 1973).
6. See R. D. Evans, The Atomic Nucleus, (McGraw Hill, N.Y., 1955) Chapter 23.
7. W. Bambynek, B. Craseman, R. W. Fink, H. U. Freund, H. Mark, C. B. Swift, R. E. Price and P. V. Rao, Rev. Mod. Phys., 44 1 (1972).
8. F. Biggs and R. Lighthill, Sandia Laboratories Report SC-RR-71-0507, (December 1971).
9. H. Brysk and C. D. Zerby, Phys. Rev. 171, 292 (1968).
10. J. W. Weymouth, Phys. Rev., 84 766 (1951).
11. T. A. Dellin, to be published.
12. L. V. Spencer, NBS Monograph 1, (1959).
13. E. A. Burke, J. A. Wall and A. R. Frederickson, IEEE Trans. Nucl. Sci., NS-17 193 (1970).
14. E. Storm and H. I. Israel, Los Alamos Report LA-3753, (June 1967).

4